High spin states in ^{151,153}Pr, ^{157}Sm, and ^{93}Kr

J. K. Hwang,[1] A. V. Ramayya,[1] J. H. Hamilton,[1] S. H. Liu,[1] N. T. Brewer,[1] Y. X. Luo,[1,2] J. O. Rasmussen,[2] S. J. Zhu,[1,3] and R. Donangelo[4,5]

[1]*Physics Department, Vanderbilt University, Nashville, Tennessee 37235, USA*
[2]*Lawrence Berkeley National Laboratory, Berkeley, California 94720, USA*
[3]*Department of Physics, Tsinghua University, Beijing 100084, Peoples Republic of China*
[4]*Instituto de Fisica, Universidade Federal do Rio de Janeiro, 21941-972 Rio de Janeiro, Brazil*
[5]*Instituto de Fisica, Facultad de Ingenieria, 11300 Montevideo, Uruguay*

(Received 7 June 2010; revised manuscript received 30 July 2010; published 10 September 2010)

High spin states are observed for the first time in the neutron-rich nuclei ^{151,153}Pr, ^{157}Sm, and ^{93}Kr from the spontaneous fission of ^{252}Cf. Twenty new transitions in ^{151}Pr, twelve in ^{153}Pr, five in ^{157}Sm, and four in ^{93}Kr were identified by using x-ray(Pr/Sm)-γ-γ and γ-γ-γ triple coincidences. From the measured total internal conversion coefficients α_T of four low-energy transitions in ^{151,153}Pr, we determine that two bands in each nucleus have opposite parity. The interlacing $E1$ transitions between the bands suggest a form of parity doubling in ^{151,153}Pr. New bands in ^{157}Sm and ^{93}Kr are reported. The half-life of the 354.8 keV state in ^{93}Kr is measured to be 10(2) ns.

DOI: 10.1103/PhysRevC.82.034308 PACS number(s): 21.10.−k, 25.85.Ca, 27.70.+q, 21.60.Cs

I. INTRODUCTION

High spin states of the odd-mass La [1,2], Ce [3–5], Nd [6,7], and Sm [8–11] isotopes around $A = 150$ have been actively studied to see whether octupole correlations exist in those isotopes. The octupole correlations in this nuclear region are based on observed parity doublets associated with the $\Delta N = 1$, $\Delta j = 3$, and $\Delta l = 3$ orbital pairs such as $\pi d_{5/2}$-$h_{11/2}$ near $Z = 56$ and $\nu f_{7/2}$-$i_{13/2}$ near $N = 88$ [12]. The ^{151,153}Pr nuclei have $N = 92$ and 94, respectively, and $Z = 59$ which are near the octupole shell gaps. The $\pi d_{5/2}3/2[411]$-$h_{11/2}3/2[541]$ and $\nu f_{7/2}3/2[532]$-$i_{13/2}3/2[651]$ Nilsson orbitals can play an important role in generating octupole shape tendencies in Pr isotopes. When the odd proton in ^{151,153}Pr occupies the $\pi h_{11/2}3/2[541]$ orbital near the Fermi surface, the octupole correlations are enhanced, because there are strong $Y_{3\mu}$ matrix elements connecting these orbitals. Parity-doublet bands indicating strong octupole correlations have not been observed in ^{149,151}Ce [13,14] and ^{149,150}Pr [15]. Therefore, it was of interest to search for the parity-doublet bands which could indicate octupole correlations in ^{151,153}Pr. For the ^{152,153}Pr isotopes, no excited states were previously known [16]. Only the first excited state in ^{150}Pr was observed from the β^- decay of ^{150}Ce [16]. Several states in ^{151}Pr were reported from the β^- decay of ^{151}Ce [17].

Since yields [18] of $^{149-152}$Pr isotopes produced from the spontaneous fission (SF) of ^{252}Cf are relatively large, SF research with ^{252}Cf becomes a good experimental method to search for high spin states in $^{149-152}$Pr. Several γ transitions in ^{151}Pr [4,15,17,19] were previously reported. The 96.8 keV transition was assigned to ^{151}Pr from the x-γ coincidences from the fission fragments of ^{252}Cf and from the β^- decay of ^{151}Ce [16,19]. Based on this 96.8 keV transition (the 96.0 keV transition in Ref. [15]), many high spin states and γ transitions were assigned to ^{151}Pr from the SF work with ^{252}Cf [15]. However, recently this 96.8 keV transition was not confirmed in the β^- decay work with Ce using the ^{235}U$(n_{\rm th}, f)$ reaction [17]. This discrepancy is solved in the present work by changing the mass of the 96.8 keV transition (the 96.0 keV transition in Ref. [15]) and its coincident transitions from ^{151}Pr to ^{150}Pr. In other words, a mass number of the previously reported bands in Ref. [15] is changed from ^{151}Pr to ^{150}Pr by comparing with the current new bands observed in ^{151,153}Pr. High spin states in ^{151}Pr and ^{153}Pr are for the first time established in the present work. These new bands are found to be parity-doublet bands that indicate the presence of the octupole correlations.

The high spin states of strongly deformed Sm and Nd nuclei [20–24] close to $A = 160$ have been actively studied from the SF works with ^{252}Cf because collective rotational bands and isomeric excited states have been predicted theoretically. The $5/2^-[523]$ and the $11/2^-[505]$ neutron bands were identified in ^{159}Sm [21,22]. Also, the $5/2^+[642]$ and $3/2^-[521]$ neutron rotational bands were observed in ^{153,155}Nd [23,24]. The $3/2^-[521]$, $5/2^+[642]$, and $5/2^-[523]$ bands were observed in the $N = 95$ isotopes of ^{159}Gd and ^{161}Dy [16]. Because these bands are missing in ^{157}Sm, the search for these neutron rotational bands in ^{157}Sm will be interesting for the systematic interpretation of the nuclear band structure. In the present work, a new band in ^{157}Sm is observed, but the configuration is not assigned. Also, four new transitions in ^{93}Kr are identified and the half-life of the 354.8 keV state measured.

II. EXPERIMENTAL METHOD

The experiment was carried out with a ^{252}Cf source of strength ≈62 μCi for two weeks by using the 101 Ge detectors of the Gammasphere. The ^{252}Cf source was sandwiched between two Fe foils of thickness 10 mg/cm^2 and was mounted in a 7.62 cm diameter plastic (CH) ball to absorb β rays, conversion electrons, and partially neutrons. The 5.7×10^{11} triple- and higher-fold γ coincidence events were obtained within a 1 μs electronic time window. The cutoff energy in the low-energy region is 33 keV. The x(Pr/Sm)-γ-γ [25] and

γ-γ-γ coincidence data were analyzed with the RADWARE software package [26].

III. RESULTS AND DISCUSSION

A. ^{151,153}Pr

In the coincidence spectra double gated on several known transitions in $^{96-99}$Y, we found the new 292.0 and 363.3 keV transitions. Because the Pr K_α and K_β x rays and transitions belonging to the Y isotopes (partner isotopes of Pr) [16] are observed in the coincidence spectrum of Fig. 1(a), these new 292.0 and 363.3 keV transitions should belong to one of the Pr isotopes. The new 206.6 and 279.5 keV transitions in Fig. 1(b) should belong to one of the Pr isotopes because the Pr K_α and K_β x rays and transitions belonging to the Y isotopes (partner isotopes of Pr) are observed in the coincidence spectrum of Fig. 1(b). The 36.0 keV peak observed in our spectra is the result of the combination of $K_{\alpha1}$ (36.026 keV) and $K_{\alpha2}$ (35.550 keV) x rays and another at 41.1 keV is the result of the combination of $K_{\beta1}$ (40.748 keV), $K_{\beta2}$ (41.764 keV), and $K_{\beta3}$ (40.653 keV) x rays [16]. The mass numbers of the new 292.0 and 363.3 keV transitions and the new 206.6 and 279.5 keV transitions are assigned to 151 and 153, respectively, from the comparison of the 122.3 (^{96}Y), 668.8 (^{97}Y), 101.0, 119.4 (^{98}Y), and 125.3 (^{99}Y) keV transition intensities in Fig. 2 as follows.

The ^{97}Y and ^{98}Y isotopes have isomeric states at excitation energies of 667.5 keV (1.17s) and 495.8 keV (8.0 μs), respectively. When we gate on the γ transitions in Pr isotopes, the ^{97,98}Y yields populating these isomeric states directly from the fission are not known. These missing ^{97,98}Y yields cannot be obtained from the coincidence spectra gated on the Pr isotopes. Therefore, the yields of ^{97,98}Y should be bigger than those obtained from the γ transition intensities in the coincidence spectra gated on the γ transitions in Pr isotopes. Rather than measuring the relative yields, the changing pattern of the γ transition intensities belonging to the Y isotopes in Fig. 2 are compared between the coincidence spectra double gated on the γ transitions belonging to ^{149,150,151,153}Pr.

For example, to assign the mass number to the new transitions, the intensity ratio values R(119.4/122.3) of the 119.4 keV (^{98}Y) and 122.3 keV (^{96}Y) transitions are compared in Fig. 3. The relative intensities of the 119.4 keV (^{98}Y) and 122.3 keV (^{96}Y) transitions are obtained from the three coincidence spectra in Fig. 2. The R(119.4/122.3) values for the Pr isotopes are 1.86(19), 0.95(10), and 0.15 (3) for Figs. 2(c), 2(b), and 2(a), respectively. In Fig. 3, the R value of 1.86(19) for Pr is normalized to the $R(4n/6n)$ value for ^{156}Sm for the comparison. The normalized R values for Figs. 2(c), 2(b), and 2(a) are 0.87(9), 0.44(4), and 0.07(1), respectively. These normalized R values for Pr are compared with the R values of $R(4n/6n) = 0.87(9)$, $R(3n/5n) = 0.47(5)$, $R(2n/4n) = 0.22(4)$, and $R(1n/3n) = 0.11(2)$ for Sm isotopes. Therefore, the normalized R(119.4/122.3) values of 0.87(9), 0.44(4), and 0.07(1) for Figs. 2(c), 2(b), and 2(a) should correspond to ^{150}Pr, ^{151}Pr, and ^{153}Pr, respectively, as shown in Fig. 3. Based on this analysis, the 155.6 and 303.7 keV transitions, 292.0 and 363.3 keV transitions, and 206.6 and 279.5 keV transitions belong to ^{150}Pr, ^{151}Pr, and ^{153}Pr, respectively. This indicates that the mass number of the previously reported bands including the 177.6 and 303.7 keV transitions [15] in Fig. 2(c) should be changed from ^{151}Pr to ^{150}Pr. This new mass assignment requires a new interpretation of the ^{150}Pr level structures and new spin and parity assignments for these levels. The 220.3 and 415.8 keV

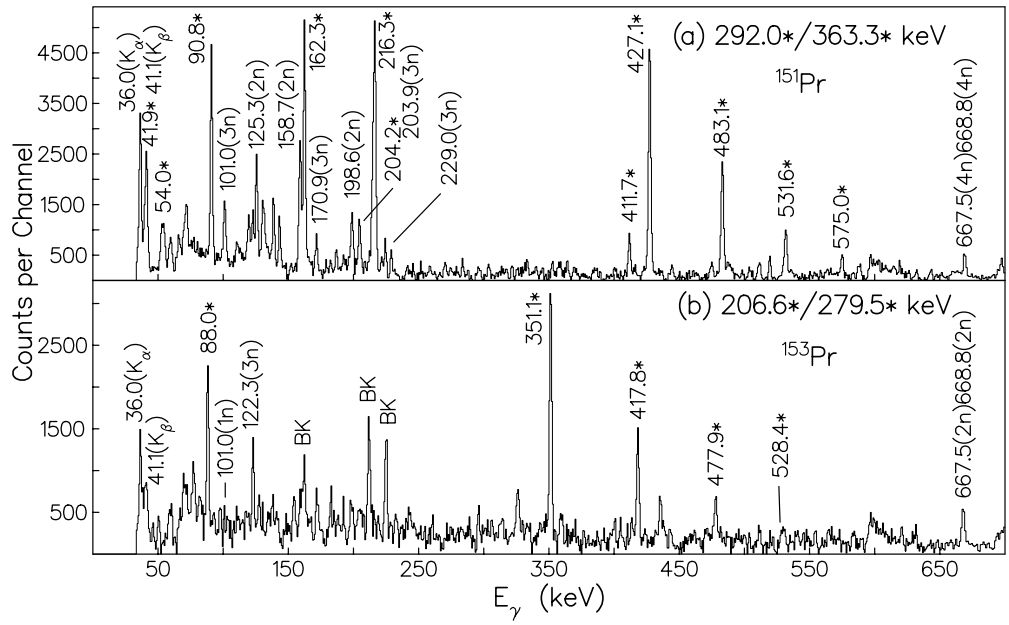

FIG. 1. Coincidence spectra double gated on the new transitions belonging to ^{151,153}Pr. Transitions marked with the asterisk are new and belong to ^{151}Pr or ^{153}Pr. 3n means the Y nucleus corresponding to the 3n channel. Note that the 101.0 keV peak (^{98}Y) in panel (b) is very weak as expected for the 1n channel. BK indicates background peaks.

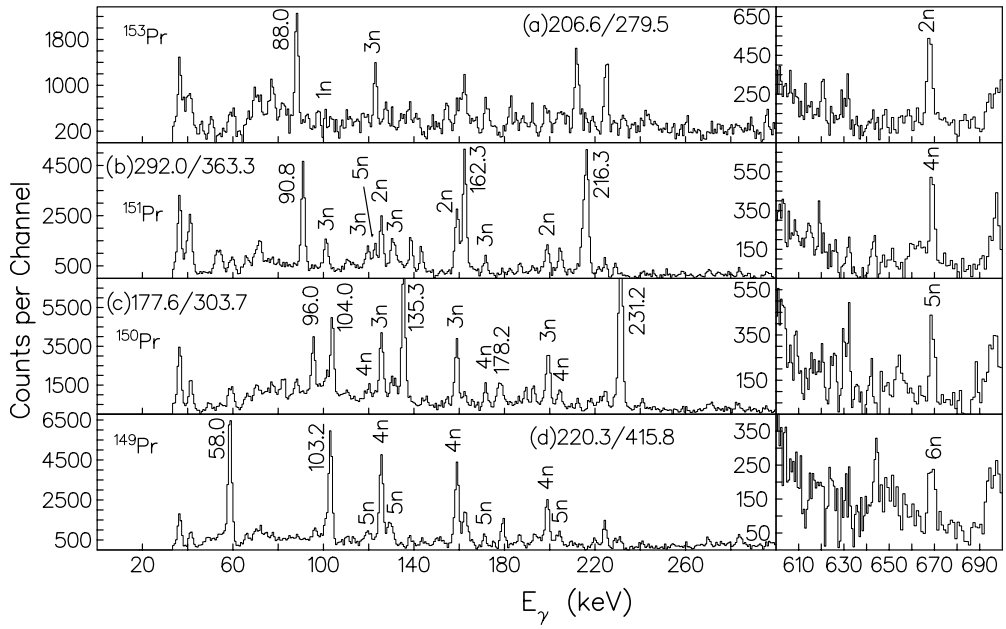

FIG. 2. Coincidence spectra double gated on the γ transitions belonging to ^{149,150,151,153}Pr. $3n$ means the Y nucleus corresponding to the $3n$ channel. The transition energy of 177.9 keV (^{150}Pr) given in Ref. [15] is changed to 177.6 keV (^{150}Pr) in the present work. Note that, in the present work, the mass number of the previously reported bands in Ref. [15] is changed from ^{151}Pr to ^{150}Pr by comparing with the current new bands observed in ^{151,153}Pr.

transitions in Fig. 2(d) should belong to ^{149}Pr as reported in Ref. [15] because the transitions corresponding to the $4n$ channel are very strong in Fig. 2(d). New transitions associated with ^{150,152}Pr will be presented in a separate publication.

From this mass assignment, in Fig. 2(a), the 122.3 keV peak ($3n$,^{96}Y) and the 668.8 keV peak ($2n$,^{97}Y) have the strengths expected for the $3n$ channel and $2n$ channel, respectively. Here the 3 neutron channel means the 3 neutron-loss channel in the spontaneous fission of ^{252}Cf. In Fig. 2(b), the 122.3 keV peak (^{96}Y) is as strong as the 119.4 keV ($3n$,^{98}Y) peak as expected for the $5n$ channel. In Fig. 2(c), the 122.3 keV peak

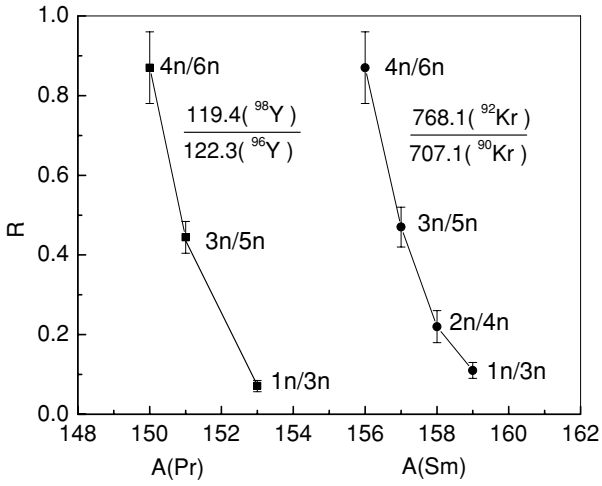

FIG. 3. Transition intensity ratios 119.4(^{98}Y)/122.3(^{96}Y) and 768.1(^{92}Kr)/707.1(^{90}Kr) as observed in Figs. 2 and 7 vs the mass numbers (A) of Pr and Sm isotopes. The $R(4n/6n)$ value for ^{150}Pr is normalized to the $R(4n/6n)$ value for ^{156}Sm for the comparison.

is much weaker than the 101.0 and 119.4 keV ($4n$,^{98}Y) and 125.3 keV ($3n$,^{99}Y) transitions as expected for the $6n$ channel. In summary, in Fig. 2(c), the 101.0, and 119.4, and 130.0 keV peaks (^{98}Y) are in the $4n$ channel and the 125.3, 158.7, and 198.6 keV peaks (^{99}Y) are in the $3n$ channel. In Fig. 3(b), the 101.0, 119.4, and 130.0 keV peaks (^{98}Y) are in the $3n$ channel, and the 125.3, 158.7, and 198.6 keV peaks (^{99}Y) are in the $2n$ channel. In Fig. 2(d), the 125.3 keV peak ($4n$,^{99}Y) is the strongest one as expected for the $4n$ channel, and the 101.0, 119.4, and 130.0 keV peaks ($5n$,^{98}Y) are relatively weak.

The new level schemes of ^{151,153}Pr in Fig. 4 are built based on the coincidence relationship of other new transitions with two new 292.0 and 363.3 keV transitions in ^{151}Pr and two new 206.6 and 279.5 keV transitions in ^{153}Pr as shown in Fig. 1. For example, twelve new transitions of energies, 41.9, 90.8, 162.3, 204.2, 216.3, 292.0, 363.3, 411.7, 427.1, 483.1, 531.6, and 575.0 keV in ^{151}Pr are identified in Fig. 1(a) and seven new transitions of energies, 88.0, 206.6, 279.5, 351.1, 417.8, 477.9, and 528.4 keV in ^{153}Pr are observed in Fig. 1(b). The low-lying excited levels in ^{150,151}Pr identified from the β^- decay work are not connected to the γ transitions observed in the present fission work of ^{252}Cf. If the lowest lying states in the ^{150,151}Pr observed from the spontaneous fission of ^{252}Cf are the ground states or isomeric states or decay through very low energy ($\leqslant$33 keV) transitions to the ground state or isomeric states, the low-lying transitions shown from the β^- decay cannot be observed. This will explain why γ transitions of ^{150,151}Pr observed in the β^- decay work are not seen in the fission work.

The total internal conversion coefficients (α_T) of the low-energy $\Delta I = 1$ transitions in Table I were obtained by comparing the transition intensities as follows. The transition

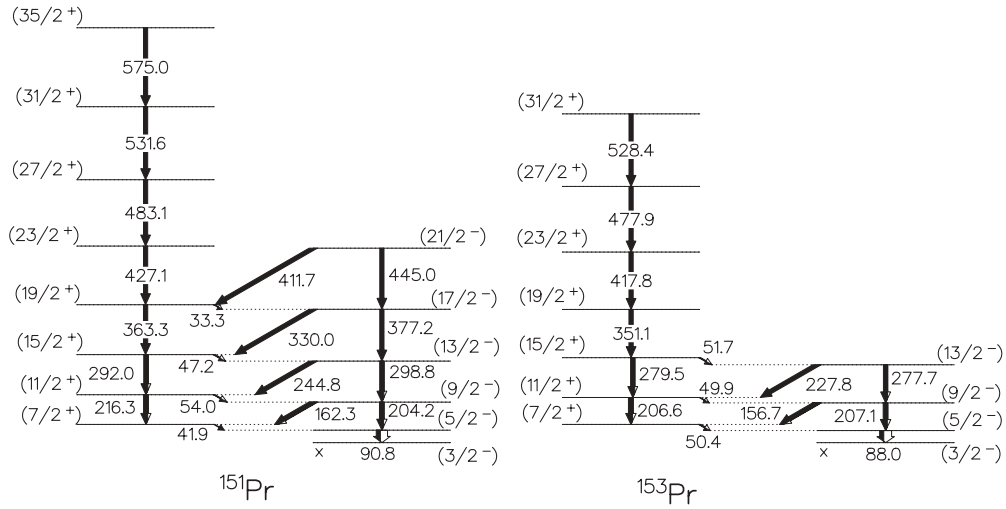

FIG. 4. New level schemes in ^{151,153}Pr. All transitions in ^{151,153}Pr are new. Note that the bandhead spin and parity $(3/2^-)$ of the parity-doublet band in ^{151}Pr is consistent with the spin and parity $(3/2^-)$ of the ground state in ^{151}Pr observed from the β^- decay work [16]. However, the parities of all four bands might be the reverse. In that case, the spin 7/2 bandhead could be the result of the strong Coriolis mixing of the lower-lying $h_{11/2}$ proton orbitals. This would be a case of semidecoupling of the odd-proton $h_{11/2}$ from the prolate spheroidal long axis.

intensities were corrected by the detection efficiency values obtained from the present fission data. The $\alpha_{\rm expt}$ value of the 54.0 keV transition was obtained from the 54.0, 162.3, and 204.2 keV transition intensities in the coincidence spectrum [Fig. 1(a)] double gated on the 292.0 and 363.3 keV transitions in ^{151}Pr. As shown in Table I, because the theoretical α_T values of the 54.0 keV transition are $\alpha_{\rm theor}(E1) = 1.34$ and $\alpha_{\rm theor}(M1) = 7.93$, if the 54.0 keV transition had an $M1$ character, the photopeak of the 54.0 keV transition should not be seen in the coincidence spectra. Since the 54.0 keV transition appears both in Fig. 1(a) and Fig. 5, the 54.0 keV transition should have an $E1$ character. The α_T value [$\alpha_{\rm theor}(E1) = 0.064$] of the 162.3 keV transition is ignored because it is small compared to the α_T value of the 54.0 keV transition. Then, the obtained α_T value [$\alpha_{\rm expt} = 1.9(6)$] of the 54.0 keV transition is only consistent with $\alpha_{\rm theor}(E1) = 1.34$ in Table I. Therefore, the 54.0 keV transition has an $E1$ character. The $\alpha_{\rm expt}$ value of the 47.2 keV transition was obtained from the 47.2, 244.8, and 298.8 keV transition intensities in the coincidence spectrum (Fig. 5) double gated on the 363.3 and 427.1 keV transitions in ^{151}Pr. As shown in Table I, because the theoretical α_T values of the 47.2 keV transition are $\alpha_{\rm theor}(E1) = 1.90$ and $\alpha_{\rm theor}(M1) = 11.8$, if the 47.2 keV transition had an $M1$ character, the photopeak of the 47.2 keV transition should not be seen in the coincidence spectra. Because the 47.2 keV transition is seen in Fig. 5, the 47.2 keV transition must have an $E1$ character. The α_T value [$\alpha_{\rm theor}(E1) = 0.0221$] of the 244.8 keV transition is ignored because it is small compared to the α_T value of the 47.2 keV transition. Then, the obtained α_T value [$\alpha_{\rm expt} = 1.2(4)$] of the 47.2 keV transition is consistent with $\alpha_{\rm theor}(E1) = 1.90$ in Table I. Therefore, the 47.2 keV transition has an $E1$ character. The $\alpha_{\rm expt}$ value of the 90.8 keV transition was obtained from the 90.8 and 292.0 keV transition intensities in the coincidence spectrum double gated on the 216.3 and 363.3 keV transitions in ^{151}Pr. Then, the obtained α_T value [$\alpha_{\rm expt} = 1.1(3)$] of the 90.8 keV transition is consistent with $\alpha_{\rm theor}(M1) = 1.75$ in Table I. The $E2$ mixing will be small because $\alpha_{\rm theor}(E2)$ is 3.03. Therefore, the 90.8 keV transition has an $M1$ character. The $\alpha_{\rm expt}$ value of the 50.4 keV transition in ^{152}Pr was obtained from the 50.4 and 279.5 keV transition intensities in the coincidence spectrum double gated on the 206.6 and 351.1 keV transitions in ^{153}Pr. Then, the obtained α_T value [$\alpha_{\rm expt} = 2.3(7)$] of the 50.4 keV transition is consistent only with $\alpha_{\rm theor}(E1) = 1.60$ in Table I. Therefore, the 50.4 keV transition has an $E1$ character.

The $\alpha_{\rm expt}$ value of the 88.0 keV transition in ^{153}Pr was obtained from the 88.0 and 279.5 keV transition intensities in the coincidence spectrum double gated on the 206.6 and 351.1 keV transitions in ^{153}Pr. Then, the obtained α_T value [$\alpha_{\rm expt} = 1.2(5)$] of the 88.0 keV transition is more consistent with $\alpha_{\rm theor}(M1) = 1.92$ in Table I. The $E2$ mixing will be small, because $\alpha_{\rm theor}(E2)$ is 3.40. Therefore, the 88.0 keV transition has an $M1$ character. The $M1$ characters of the 90.8 keV (^{151}Pr) and 88.0 keV (^{153}Pr) explain why the crossover 132.7 keV (^{151}Pr) and 138.4 keV (^{153}Pr) transitions are missing in Fig. 4. It is because the crossover 132.7 keV (^{151}Pr) and 138.4 keV (^{153}Pr) transitions would be $M2$ transitions in Fig. 4. Based on

TABLE I. Total internal conversion coefficients (α_T) of the low-energy transitions in ^{151}Pr and ^{153}Pr.

Nucleus	Energy	$\alpha_{\rm expt}$	$\alpha_{\rm theor}$		
			$E1$	$M1$	$E2$
^{151}Pr	47.2	1.2(4)	1.90	11.8	37.5
	54.0	1.9(6)	1.34	7.93	21.8
	90.8	1.1(3)	0.328	1.75	3.03
^{153}Pr	88.0	1.2(5)	0.358	1.92	3.40
	50.4	2.3(7)	1.60	9.71	28.7

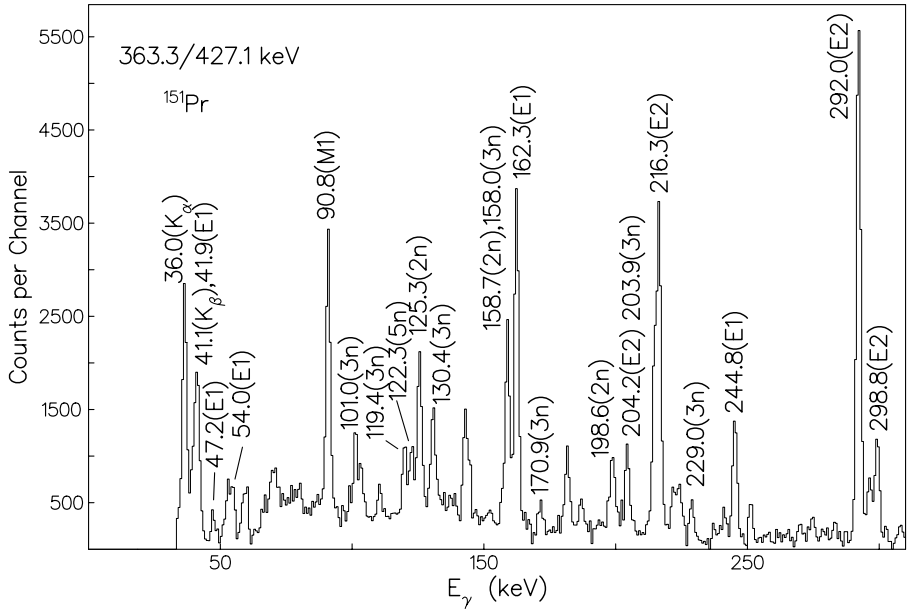

FIG. 5. Coincidence spectrum double gated on the 363.3 and 427.1 keV transitions in ^{151}Pr.

these measurements, all other $\Delta I = 1$ transitions of the new bands except the 90.8 keV transition in ^{151}Pr and 88.0 keV transition in ^{153}Pr have an $E1$ character. It is suggested that the new bands in ^{151,153}Pr are parity-doublet bands because of the intertwined $E1$ transitions.

In Table II, the $B(E1)/B(E2)$ values shown are calculated from the equation $\frac{B(E1)}{B(E2)} = 0.771 \frac{I_\gamma(E1)E_\gamma(E2)^5}{I_\gamma(E2)E_\gamma(E1)^3}$ (10^{-6} fm^{-2}) for Weisskopf units $\frac{B_W(E1)}{B_W(E2)} = 3.84 \times 10^{-2}$ fm^{-2} for Pr. The $B(E1)/B(E2)$ ratios for the low-energy $E1$ transitions at 47.2 and 54.0 keV are much larger than other $B(E1)/B(E2)$ ratios. Based on the systematics, it has been known that for deformed nuclei with $A \approx 150$, the $E2$ transition strength is enhanced by a factor of up to 300–1000, while the $E1$ transition strength is reduced by a factor of around 0.01 from the Weisskopf single-particle shell-model calculated value [16]. Therefore the systematic $B(E1)/B(E2)$ values are around 10^{-5} W.u. This estimate was obtained from experimental data including $E1$ transition energies between 100 and 200 keV. In Table II, the $B(E1)/B(E2)$ values including the higher energy $E1$ transitions at 330.1, 244.8, and 162.3 keV are consistent with the systematic estimate above. The $B(E1)/B(E2)$ values including the lower energy $E1$ transitions at 47.2 and 54.0 keV are an order of 10 larger than the systematic value. These large $B(E1)/B(E2)$ values may indicate relatively reduced quadrupole collectivity (in other words, increased single-particle characteristics) as well as enhanced octupole correlations caused by the odd-proton of ^{151,153}Pr. In order to analyze the $B(E1)/B(E2)$ values systematically, more experimental data of the odd-odd and odd-A nuclei in the $A = 150$–170 region are required, especially for the low-energy $E1$ transitions around 50 keV. A comparison with microscopic calculations could shed more light on the mechanism responsible for the enhanced $E1$ strength.

TABLE II. $B(E1; I-1)/B(E2; I-2)$ ratios in ^{151}Pr.

Energy	$B(E1)/B(E2)$		Energy	$B(E1)/B(E2)$	
	10^{-6} fm^{-2}	10^{-6} W.u.		10^{-5} fm^{-2}	10^{-4} W.u.
330.0/377.2	0.34(8)	8.9(21)	47.2/292.0	3.2(10)	8.3(26)
244.8/298.8	0.16(4)	4.2(10)	54.0/216.3	0.92(33)	2.4(9)
162.3/204.2	0.26(6)	6.8(16)			

There are $\pi d_{5/2}3/2[411]$-$h_{11/2}3/2[541]$ and $\nu f_{7/2}3/2[532]$-$i_{13/2}3/2[651]$ Nilsson orbitals which can play an important role in promoting octupole collectivity in Pr isotopes. In ^{151,153}Pr, if the odd proton occupies the $\pi h_{11/2}3/2[541]$ orbital associated with the octupole correlation, the observed parity-doublet bands could be explained. In this case, the bandhead state would be assigned spin-parity $3/2^-$. This proposed bandhead spin-parity of the parity-doublet bands in ^{151}Pr($3/2^-$) are consistent with the tentative ground-state spin-parity ($3/2^-$) of ^{151}Pr deduced from β^- decay of ^{151}Ce [16,17]. A transition from the 132.7 keV $7/2^+$ level to a tentative ($7/2^+$) level at 35.1 keV seen in ^{151}Pr from β^- decay was not seen. Based on other cases where octupole doublets are seen along with other states, e.g., ^{145}Ba [27], one would not expect to see this $(7/2^+) \rightarrow (3/2^+)$ decay because of their different structure. The spin-parity of the ground state of ^{153}Pr was not previously known.

B. ^{157}Sm and ^{93}Kr

The production yield of ^{157}Sm is 0.277 per 100 ^{252}Cf spontaneous fission (SF) events [18]. The intensities of the γ transitions in ^{157}Sm are weak. Therefore, the x-ray(Sm)-γ-γ triple coincidences [25] were mainly used to confirm these weak transitions. It is shown in Fig. 6 that the new 273.8 and 348.6 keV transitions are in coincidence with Sm x rays. The 40.1 keV peak observed in our spectra is the result of the combination of $K_{\alpha 1}$ (40.118 keV) and $K_{\alpha 2}$ (39.522 keV) x rays and another at 45.8 keV is the result of the combination of $K_{\beta 1}$ (45.414 keV), $K_{\beta 2}$ (46.578 keV), and $K_{\beta 3}$ (45.293 keV)

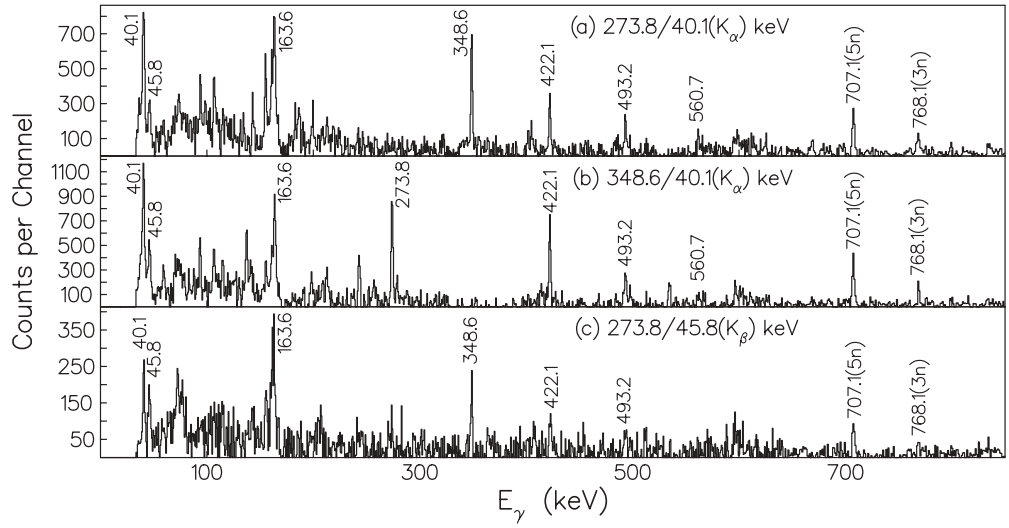

FIG. 6. Coincidence spectra double gated on the γ transitions in ^{157}Sm and the Sm x rays. 5*n* means the Kr nucleus corresponding to the 5*n* channel.

x rays [16]. Because the 40.1 and 45.8 keV x(Sm) rays are the combination of two and three main x rays, the 40.1 and 45.8 keV x(Sm)-ray peaks are still seen in the spectra in Fig. 6, even though these are gated by the 40.1 (K_α) and 45.8 (K_β) keV x rays of Sm. To separate the background peaks from the real coincident peaks, three coincidence spectra are shown in Fig. 6. Real coincident transitions of energies 163.6, 273.8, 348.6, 422.1, 493.2, and 560.7 keV appear in all three spectra in Fig. 6. Also, because the 707.1 keV (^{90}Kr) and 768.1 keV (^{92}Kr) transitions of the Kr nuclei (Sm fission partner) are observed in the three spectra in Fig. 6, the transitions of energies 163.6, 273.8, 348.6, 422.1, 493.2, and 560.7 keV should belong to one of the Sm isotopes. In Fig. 6(a), double gated on the 273.8 keV transition and the 40.1 keV x ray, the 707.1 keV (^{90}Kr) and 768.1 keV (^{92}Kr) transitions are clearly seen.

To assign the mass number to these new transitions, the intensity ratio values R(768.1/707.1) of the 707.1 keV (^{90}Kr) and 768.1 keV (^{92}Kr) transitions are compared in Fig. 3. The relative intensities of the 707.1 keV (^{90}Kr) and 768.1 keV (^{92}Kr) transitions are obtained from the four coincidence spectra in Fig. 7. The R(768.1/707.1) values are 0.87(9), 0.22(4), and 0.11 (2) for ^{156}Sm, ^{158}Sm, and ^{159}Sm, respectively. The R(768.1/707.1) value in the coincidence spectrum [Fig. 7(b)] gated on the new 273.8 keV transition is 0.47(5) which, as shown in Fig. 3, should correspond to ^{157}Sm. Therefore, the transitions of energies 163.6, 273.8, 348.6, 422.1, 493.2, and 560.7 keV should belong to ^{157}Sm. The new level scheme of

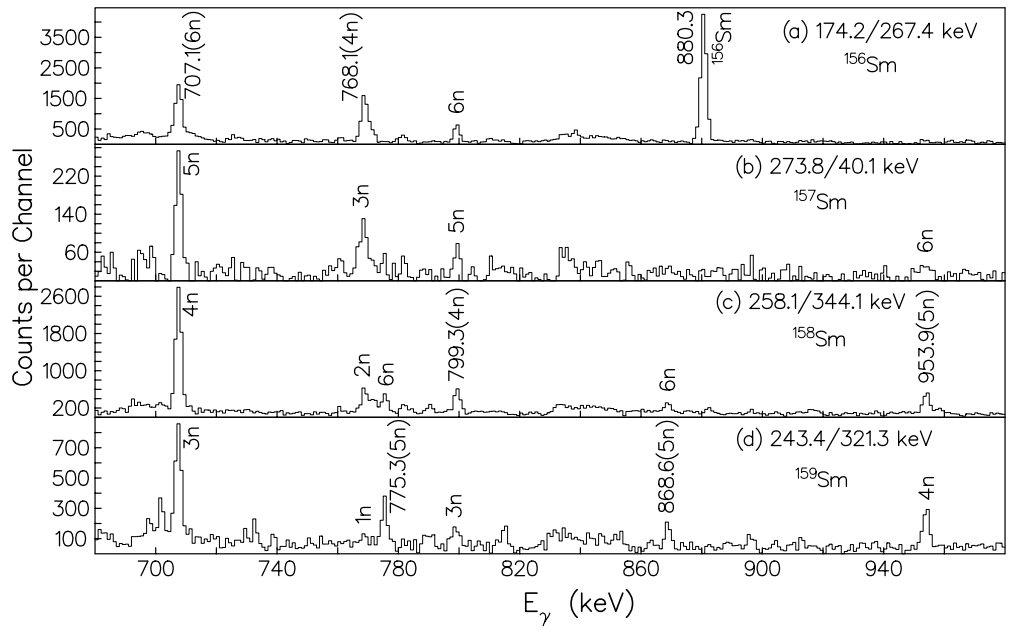

FIG. 7. Spectra in coincidence with transitions in ^{156,157,158,159}Sm. 5*n* means the Kr nucleus corresponding to the 5*n* channel.

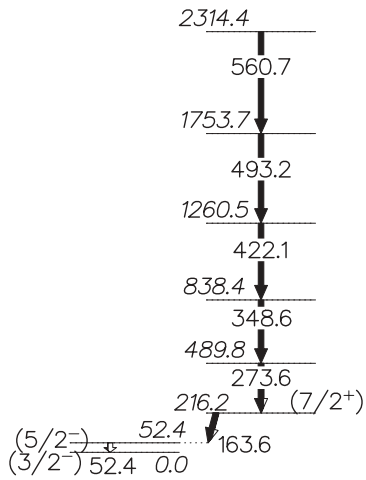

FIG. 8. New level schemes for ^{157}Sm. The 273.8, 348.6, 422.1, 493.2 and 560.7 keV transitions in ^{157}Sm are new. Gamma transitions below the $(7/2^+)$ state were previously known from β^- decay work [16].

^{157}Sm is shown in Fig. 8. The 52.4 and 163.6 keV transition were previously known from β^- decay work [16]. Because the band observed in ^{157}Sm is very weakly populated, the γ transitions belonging to the partner Kr isotopes are not seen in the coincidence spectra in Fig. 6. Very weak transitions below the $7/2^+$ state reported from the β^- decay work [16] were not clearly observed in the present fission work. Therefore, these transitions are not shown in the partial level scheme (Fig. 8) of ^{157}Sm.

The 117.4 and 237.4 keV transitions in ^{93}Kr were observed by G. Lhersonneau *et al.* from ^{93}Br β^--decay data [28]. More recently, Simpson *et al.* [29] put a new 237.8 keV transition above the 117.8 keV transition [30] in the ^{156}Sm level scheme based on the coincidence spectrum double gated on 1147.7 and 174.2 keV transitions in ^{156}Sm. However, the 117.4 and 237.4 keV transitions in ^{93}Kr should be seen in this coincidence spectrum in the $3n$ channel, but in Ref. [29] the ^{93}Kr transitions were not noticed, and they were not marked with asterisks in Fig. 6 of Ref. [29]. Also, we have confirmed that the 117.4 and 237.4 keV transitions belong to ^{93}Kr in the coincidence spectrum double gated on the 174.2 and 354.5 keV transitions in ^{156}Sm. In this coincidence spectrum, the previously known [30] 117.8 keV transition in ^{156}Sm is excluded. In fact, from the coincidence spectra double gated on one γ transition in ^{156}Sm (174.2, 267.4, 1147.7, or 117.8 keV) and another γ transition in ^{90}Kr (707.1 keV) or ^{92}Kr (768.1 keV), it was confirmed that the 117.8 keV transition in ^{156}Sm reported from the β^- decay of ^{156}Pm [30] is negligibly weak, so it could not be observed in the present work. Therefore, the 237.4 keV transition should not belong to ^{156}Sm but to ^{93}Kr. In the coincidence spectrum (Fig. 9) double gated on the 237.4 and 628.4 keV transitions in ^{93}Kr, the 174.2 and 267.4 keV transitions belonging to ^{156}Sm are shown in the $3n$ channel, but no Kr transitions such as the 768.1 keV transition in ^{92}Kr and the 707.1 keV transition in ^{90}Kr appear, as expected for the coincidence spectrum double gated on the Kr transitions. Then by gating on two known transitions of energies, 117.4 and 237.4 keV, four new transitions of energies, 628.4, 533.7, 884.8, and 798.1 keV were identified in ^{93}Kr (see Fig. 9). The new level scheme for ^{93}Kr is shown in Fig. 10.

In the present work, the half-life of the 354.8 keV state is determined to be 10(2) ns by using the γ-γ-γ coincidences with different time windows (t) [31] as follows. In Fig. 11, coincidence spectra with several different time windows (t) are compared by double gating on the 533.7 and 884.8 keV transitions. In the 8 and 16 ns coincidence spectra [Figs. 11(a) and 11(b)], count ratios of $N(237.4)/N(628.4)$ are clearly reduced when compared with the count ratios in the 28, 48, and 72 ns coincidence spectra [Figs. 11(c)–11(e)]. This

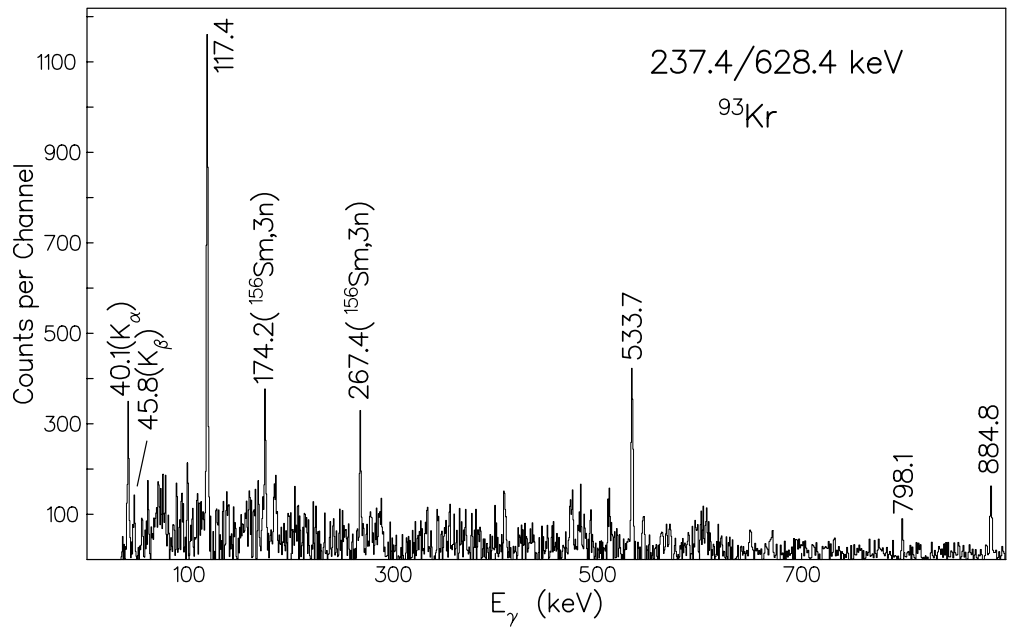

FIG. 9. Coincidence spectra double gated on the γ transitions in ^{93}Kr. K_α and K_β are Sm x rays [16].

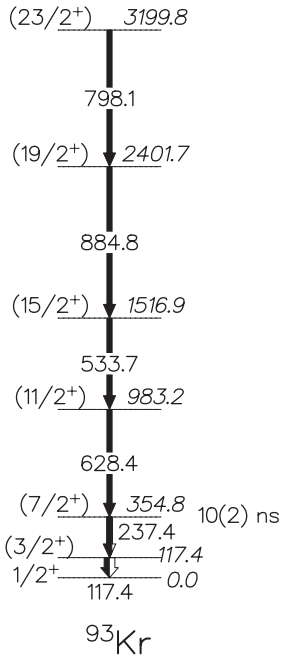

FIG. 10. New level scheme for ^{93}Kr. The 628.4, 533.7, 884.8, and 798.1 keV transitions in ^{93}Kr are new.

indicates that the 354.8 keV state between the 628.4 and 237.4 keV transitions has the half-life of about 8–16 ns. These count ratios versus t are plotted in Fig. 12 in order to determine the half-life of the 354.8 keV state. The count ratios $N(237.4)/N(628.4)$ can be fit to the decaying equation of $R = N(237.4)/N(628.4) = N_o(1 - e^{-\lambda t})$ [31] as shown in Fig. 12. The count N does not have to be corrected for the detection efficiency and internal conversion coefficient,

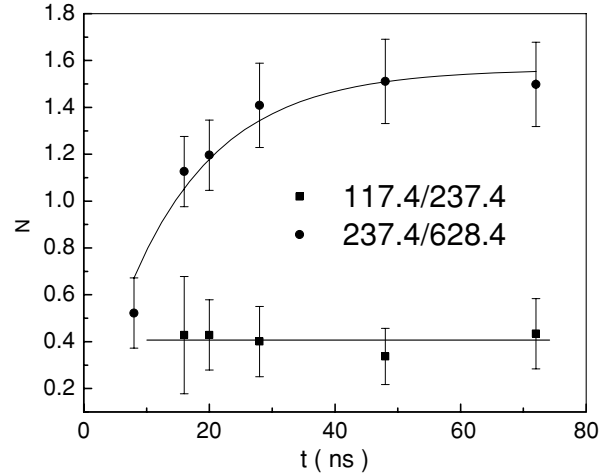

FIG. 12. Normalized counts vs time window (t) to determine the half-life.

because those constant effects are included in the coefficient of N_o. The half-life of the 354.8 keV state extracted from the observed decay constant λ is 10(2) ns, which can be compared with the previously measured half-life of 22(12) ns obtained from a $\gamma\gamma(t)$ measurement using the β^- decay of ^{93}Br [28]. In the 8 and 16 ns coincidence spectra [Figs. 11(a) and 11(b)], count ratios of $N(117.4)/N(237.4)$ are not reduced relatively when compared with the count ratios in the 28, 48, and 72 ns coincidence spectra [Figs. 11(c)–11(e)]. This means that the half-life of the 117.4 keV state has to be shorter than 4 ns, because in the 8 ns coincidence spectra the count ratio of $N(117.4)/N(237.4)$ does not show any decrease when compared with those in the 16, 28, 48, and 72 ns coincidence spectra.

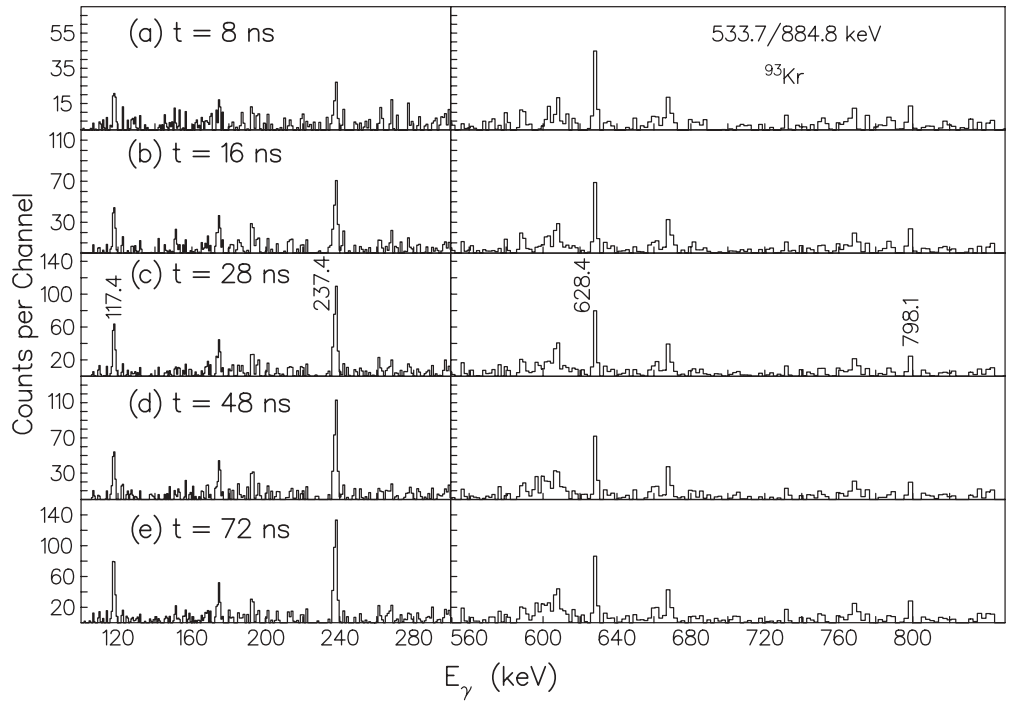

FIG. 11. Coincidence spectra with several time windows (t).

IV. CONCLUSION

In conclusion, in the present work 20 new transitions in ^{151}Pr and 12 new transitions in ^{153}Pr were identified. From total internal conversion coefficient measurements, the two bands in each of these nuclei have opposite parities. These opposite parities may indicate the influence of octupole correlations. Six and four new γ transitions were identified in ^{157}Sm and ^{93}Kr, respectively. The half-life of the 354.8 keV state in ^{93}Kr was measured to be 10(2) ns.

ACKNOWLEDGMENTS

The work at Vanderbilt University and Lawrence Berkeley National Laboratory are supported by the US Department of Energy under Grant No. DE-FG05-88ER40407 and Contract No. DE-AC03-76SF00098. The work at Tsinghua University was supported by the National Natural Science Foundation of China under Grant No. 10975082 and the Major State Basic Research Development Program 2007CB815005. R.D. acknowledges partial financial support from PEDECIBA (Uruguay) and CNPq (Brazil).

[1] S. J. Zhu *et al.*, Phys. Rev. C **59**, 1316 (1999).
[2] Y. X. Luo *et al.*, Nucl. Phys. A **818**, 121 (2009).
[3] W. R. Phillips *et al.*, Phys. Lett. B **212**, 402 (1988).
[4] S. J. Zhu *et al.*, Phys. Lett. B **357**, 273 (1995).
[5] Y. X. Luo *et al.*, Nucl. Phys. A **838**, 1 (2010).
[6] W. Urban *et al.*, Phys. Lett. B **200**, 424 (1988).
[7] H. H. Pitz *et al.*, Nucl. Phys. A **509**, 587 (1990).
[8] E. Hammaren *et al.*, Nucl. Phys. A **321**, 71 (1979).
[9] W. Urban *et al.*, Phys. Lett. B **185**, 331 (1987).
[10] W. Urban *et al.*, Phys. Lett. B **258**, 293 (1991).
[11] F. R. Metzger *et al.*, Phys. Rev. C **14**, 543 (1976).
[12] W. Nazarewicz and S. L. Tabor, Phys. Rev. C **45**, 2226 (1992).
[13] A. Syntfeld *et al.*, Nucl. Phys. A **710**, 221 (2002).
[14] G. S. Simpson *et al.*, Phy. Rev. C **81**, 024313 (2010).
[15] J. K. Hwang *et al.*, Phys. Rev. C **62**, 044303 (2000).
[16] R. B. Firestone and V. S. Shirley, *Table of Isotopes*, 8th ed. (John Wiley and Sons, New York, 1996); [www.nndc.bnl.gov].
[17] Y. Kojima *et al.*, Nucl. Instrum. Methods Phys. Res. A **564**, 275 (2006).
[18] A. C. Wahl, At. Data Nucl. Data Tables **39**, 1 (1988).
[19] B. Singh, Nucl. Data Sheets **110**, 1 (2009).
[20] J. H. Hamilton *et al.*, Prog. Part. Nucl. **35**, 635 (1995).
[21] J. K. Hwang *et al.*, Phys. Rev. C **78**, 017303 (2008).
[22] W. Urban, G. S. Simpson, A. G. Smith, J. F. Smith, T. Rzkaca-Urban, and I. Ahmad, Phys. Rev. C **80**, 037301 (2009).
[23] J. K. Hwang *et al.*, Int. J. Mod. Phys. E **6**, 331 (1997).
[24] J. K. Hwang *et al.*, Phys. Rev. C **78**, 014309 (2008).
[25] J. K. Hwang *et al.*, Phys. Rev. C **80**, 037304 (2009).
[26] D. C. Radford, Nucl. Instrum. Methods Phys. Res. A **361**, 297 (1995).
[27] S. J. Zhu *et al.*, Phys. Rev. C **60**, 051304 (1999).
[28] G. Lhersonneau, A. Wohr, B. Pfeiffer, and K. L. Kratz (ISOLDE Collaboration), Phys. Rev. C **63**, 034316 (2001).
[29] G. S. Simpson *et al.*, Phys. Rev. C **80**, 024304 (2009).
[30] M. Hellström, B. Fogelberg, L. Spanier, and H. Mach, Phys. Rev. C **41**, 2325 (1990).
[31] J. K. Hwang *et al.*, Phys. Rev. C **69**, 057301 (2004).